Poly(adenine)-mediated DNA-functionalized gold nanoparticles for sensitive detection of mercury ions in aqueous media

Jinjin Yin, Jiuchao Wang, Xiyue Yang, Tao Wu, [ID] * Huashan Wang [ID] * and Xiaoming Zhou

In this work, a facile and sensitive colorimetric sensor for Hg^{2+} ions based on poly (adenine)-mediated DNA-functionalized gold nanoparticles (Au NPs) is reported. One DNA sequence consisting of poly-A and T-rich DNA was designed rationally. Poly-A was used as an anchoring block to bind tightly to Au NPs, and T-rich DNA was utilized for specific recognition of Hg^{2+} ions. With the assistance of poly-A, T-rich DNA was easily introduced onto the surface of Au NPs and kept an upright orientation. In the presence of Hg^{2+} ions, T base binding with Hg^{2+} ions results in the formation of "T–Hg^{2+}–T" among the Au NPs, which caused aggregation of the Au NPs and a subsequent change in the color of the solution, from wine red to grayish blue. On this occasion, the limit of detection (LOD) was 3.75 nM Hg^{2+} ions with a linear range from 5 nM to 200 nM, as measured by UV-Vis spectroscopy. Moreover, successful application of this method for the detection of Hg^{2+} ions in real samples was demonstrated.

Introduction

It is generally acknowledged that mercury is one of the severest pollutants with different forms in the natural environment.[1] Mercury ions (Hg^{2+}) are the main and most widely distributed form that could be converted to organic mercury with higher toxicity by microorganisms. Organic mercury could be accumulated in organisms in the food chain and result in acute damage to human health, such as permanent damage to the central nervous system, brain and liver.[2–5] These serious health problems have encouraged researchers to develop efficient, facile and fast methods for detection of Hg^{2+} in the environment with high selectivity and sensitivity to reduce the conversion of organic mercury.[6–11] The World Health Organization has established a maximum permissible Hg^{2+} level of 5 nM in drinking water.[12] At present, the conventional analysis methods for Hg^{2+} ions with responsive sensitivity include absorption spectrometry, inductively coupled plasma-mass spectrometry and so on.[13–15] However, these methods suffer from their own disadvantages, such as complicated sample treatment, and requiring trained personnel, expensive equipment and off-site analysis.

Oligonucleotides are not only genetic material in biology, but also useful tools in chemistry, such as used as a template to prepare nano-materials[16–18] used as an element to engineer

nano-probe and used as the "chemistry antibody" to recognize targets (aptamer) and so on.[19–21] The thymine (T) base of oligonucleotide specific binding with Hg^{2+} to form "T–Hg^{2+}–T" complex, and since it was reported,[22] many sensors for detection of Hg^{2+} have been developed based on it.[23,24] Liu developed a Hg^{2+} detection method with a detection limit of 0.5 nM by using Hg^{2+} specific probe (18T) and the intercalation dye SYBR Green I.[25] In order to expand the application of detection methods, nanomaterials have been employed to construct sensitive sensors for Hg^{2+}. Gold nanoparticles (Au NPs) are widely used to engineer nano-sensors in the fields of analytical chemistry and bio-sense because of their excellent physicochemical properties.[26–28] In 2007, Mirkin developed a colorimetric detection of Hg^{2+} in aqueous media using DNA-functionalized Au NPs for the first time.[29] Furthermore, Liu reported a room temperature colorimetric method to detect Hg^{2+} based on DNA conjugated Au NPs.[30] Recently, Chen and co-workers developed a colorimetric sensor for Hg^{2+} based on "T–Hg^{2+}–T" coordination to grow Au NPs furtherly.[10]

Up to now, most DNA-functionalized Au NPs are usually thiolate-modified DNA probes on the surface of Au NPs, and it is a multi-step and time-consuming chemical process to construct them.[31,32] Fortunately, it has been reported that poly-A as an effective anchoring block could bind tightly to the surface of Au NPs, which is a facile and label-free process. Moreover, the DNA probe connected with poly-A could maintain an upright orientation, which favours the binding of the target to the DNA probe.[33,34] Based on this principle, we employed a single-stranded DNA (ssDNA) containing thymine (T)-rich DNA and poly-adenine to engineer a versatile and sensitive colorimetric

College of Chemical Engineering and Materials Science, State Key Laboratory of Food Nutrition and Safety, Key Laboratory of Food Nutrition and Safety, Tianjin University of Science and Technology, Tianjin 300457, China. E-mail: wutaoxx@gmail.com; whs@tust.edu.cn

detection method specific to Hg^{2+} ions based on Au NPs. Poly-A brings the T-rich DNA to Au NPs, and T-rich DNA strands can be hybridized with each other among the Au NPs because of Hg^{2+} ions lead to form the structure of "T–Hg^{2+}–T". Then the colour of solution of Au NPs changes when the Au NPs aggregate. The limit of detection (LOD) was measured at 3.75 nM Hg^{2+} ions using UV-Vis spectroscopy. And this strategy specific to Hg^{2+} ions cannot be affected by other metal ions. It is a facile and fast detection sensor for Hg^{2+} ions with high sensitivity and selectivity.

Experimental

Materials and chemicals

Chloroauric acid ($HAuCl_4$) was purchased from Sigma-Aldrich Chemicals. A stock solution of $HAuCl_4$ was prepared by dissolving 1.0 g $HAuCl_4$ in 100 mL ultrapure water (18.2 MΩ cm^{-1}) from a Millipore water purification system. Sodium citrate and hydrochloric acid were purchased from Sinopharm Chemical Reagent Co. Ltd. Purified DNA sequences were purchased from Sangon Biotechnology Co. Ltd (Shanghai, China) and schematically shown in Table 1. Standard liquid elemental mercury (1 mg mL^{-1}) was purchased from Aladdin Industrial Corporation. Unless otherwise noted, all reagent grade chemicals were used directly without further purification.

Preparation and characterization of Au NPs

All glassware was washed and then thorough rinsed with chloroazotic acid before use in this work. Au NPs (an average diameter of 13 nm) were prepared by the reduction of $HAuCl_4$ solution with sodium citrate.[35] Briefly, 50 mL of 1% $HAuCl_4$ solution was heated to 100 °C. Then, 10 mL sodium citrate solution (38.8 mM) was freshly prepared and added rapidly to the $HAuCl_4$ solution. The solution was mixed by stirring and heating until the colour of the solution turned to wine red. The solution was cooled naturally to room temperature and then stored at 4 °C in the dark before using. Ultraviolet-visible (UV-Vis) spectra of the Au NPs solution were characterized at 520 nm using a Cary 50-Bio UV spectrometer (Victoria, Australia). Transmission electron microscopy (TEM) images of the Au NPs were obtained with a 2010FEF microscope (JEOL, Japan).

Preparation of DNA–Au NPs conjugates

The preparation of DNA–Au NP conjugates based on poly-adenine-mediation was performed according to a procedure by Opdahl et al.[33] Briefly, Au NPs were incubated with A-rich DNA with a molar ratio of 200 (DNA : Au NPs) for 12 h on ice. The buffer used in this process was composed of 10 mM sodium phosphate and 0.1 M NaCl at pH 7.4. And then the conjugates were washed three times with this buffer at centrifugation with 12 000 rpm, 20 min, 4 °C.

Detection of Hg^{2+} by our strategy in buffer

For Hg^{2+} detection, 5 μL solution containing different concentrations of Hg^{2+} ions were incubated with 200 μL DNA–Au NPs conjugates for 10 min. And then the absorption at 520 nm was recorded by Cary 50-Bio UV spectrometer. For each sample, the experiment was repeated three times. The control experiments using 5 μL of solution without Hg^{2+} ions were carried out under same conditions.
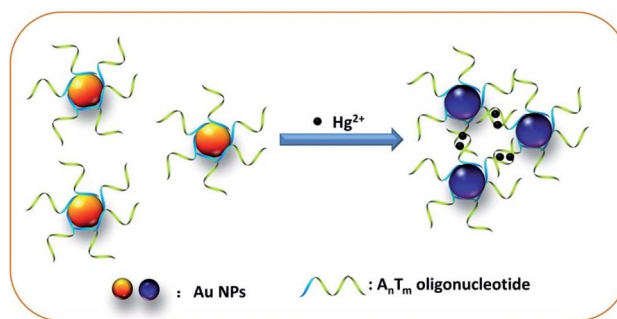
Detection of Hg^{2+} in real samples

To investigate the capability of our strategy for practical application, tap water and lake water were used as real samples in this work. The tap water was used directly without further measurement, and the lake water samples were collected from a lake located on the campus of the Tianjin University of Science and Technology, was first filtered by using a 0.22 μm membrane to remove the sand, particles and microorganisms. All the water samples were treated with different concentrations of Hg^{2+} ions on the basis of the presence of possible metal ions in the water. The detection procedure method used was mentioned above.

Results and discussion

Sensor operation principle

The colorimetric detection of mercury ions based on poly-adenine-mediated DNA-functionalized gold nanoparticles is shown in Scheme 1. This strategy relies on a well-designed ssDNA containing thymine (T)-rich DNA (in green) and poly-adenine (A) (in blue) to engineer a colorimetric strategy specific to Hg^{2+} based on Au NPs. In this design, the T-rich portion is used to discern Hg^{2+}, and poly-A portion is used as

Table 1 DNA sequences used in this work

DNA name	DNA sequences (5′–3′)
T15	TTTTTTTTTTTTTTT
A5R	AAAAA-random sequence (10 bases)
A5T15	AAAAATTTTTTTTTTTTTTTTTTTT
A5T10	AAAAATTTTTTTTTT
A5T5	AAAAATTTTT
A10T10	AAAAAAAAAATTTTTTTTTT
A15T10	AAAAAAAAAAAAAAATTTTTTTTTT
A20T10	AAAAAAAAAAAAAAAAAAAATTTTTTTTTT
A5A	AAAAATTCTTCTTTCTTCCCCCCTTGTTTGTTGTTT

Scheme 1 The principle of poly-A mediated DNA-functionalized Au NPs for sensitive detection of Hg^{2+} ions.

an anchoring block to bind with Au NPs. With the assistance of poly-A, T-rich DNA could be connected to Au NPs and maintain an upright orientation. In the presence of Hg^{2+} ions, the precise structure of "T–Hg^{2+}–T" appears in the T-rich DNA portion, which will result in aggregation of the Au NPs. In contrast, in the absence of Hg^{2+} ions, T-rich DNA portion cannot hybridize between each other and not form aggregated Au NPs. The different colored solutions of Au NPs (from wine red to grayish blue) are obtained through the generation of morphologically varied Au NPs.

Feasibility study experiment

As a proof of feasibility experiment, several DNA sequences were used with Au NPs. As shown in Fig. 1A, the curve a is the absorption spectrum of the Au NPs, curve b is the resolution of Au NPs with 1 μM Hg^{2+} ions, and curves c–e are the resolution of T15, A5R and A5T10–Au NPs with 1 μM Hg^{2+} ions, respectively. From Fig. 1A, we can find that the obvious absorption peak change appear in curve e, A5T10–Au NPs with 1 μM Hg^{2+} ions. The oligonucleotide of A5T10 is consist of poly-A and T-rich base, whereas T15 is only T-rich sequence, and A5R includes poly-A with a random base sequence. The results proved that our designed strategy specific to Hg^{2+} ions works well. Moreover, TEM images of the solution of A5T10–Au NPs with and without 1 μM Hg^{2+} ions are shown in Fig. 1B, respectively. An aggregated Au NPs were found after adding 1 μM Hg^{2+} ions in A5T10–Au NPs, which further confirmed the performance of our design.

Optimization of experimental conditions

To achieve a sensitive and selective response of the assay, several analytical parameters were investigated, including the number of adenine and thymine bases, recognition sequence, the concentration of DNA and the pH of solution. Firstly, the number of adenine and thymine bases was studied, as shown in Fig. 2. Different DNA sequences were used to anchor the Au NPs and then 5 μM Hg^{2+} ions was added. The change in the absorption peak at approximately 520 nm was recorded by UV-Vis spectroscopy. Fig. 2B shows that, the A5T10 anchored Au NPs exhibited the best response to Hg^{2+} ions in these designed DNA sequences. It should be noted that the aptamer of Hg^{2+} ions was connected with 5 adenine bases (A5A), which could change the absorption peak at approximately 520 nm of the Au NPs in the presence of Hg^{2+} ions. However, the change was not as obvious as that of A5T10 (see in Fig. 2). Thus, A5T10 was selected to engineer the strategy in this work.

In this design, because the concentration of DNA and the pH of the solution have impacts on the sensitivity of this detection strategy, we investigated the effects of different dosages of DNA and pH of the buffer. The results are shown in Fig. 3A, and indicate that when the concentration of DNA increased, the change in the absorbance at 520 nm did not increase greatly when the concentration of DNA was much more than 1 μM with 500 nM Hg^{2+} ions. We investigated the pH effects from 6.0 to 8.0, as shown in Fig. 3B. The biggest change in absorbance at 520 nm was obtained at pH 7.4. In summary, the optimum condition was 1 μM A5T10 DNA in pH 7.4 buffer.

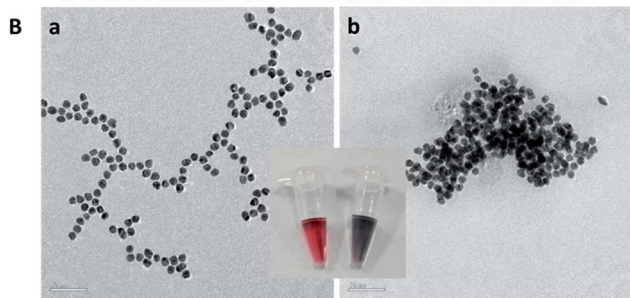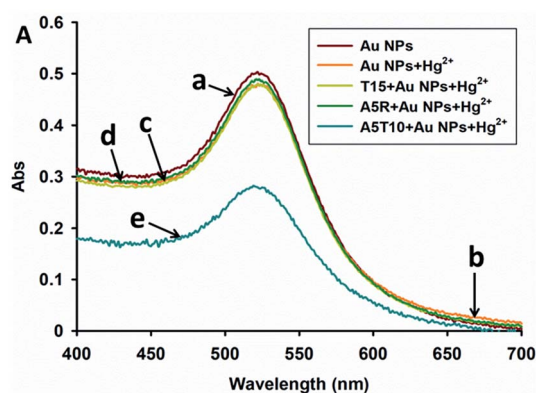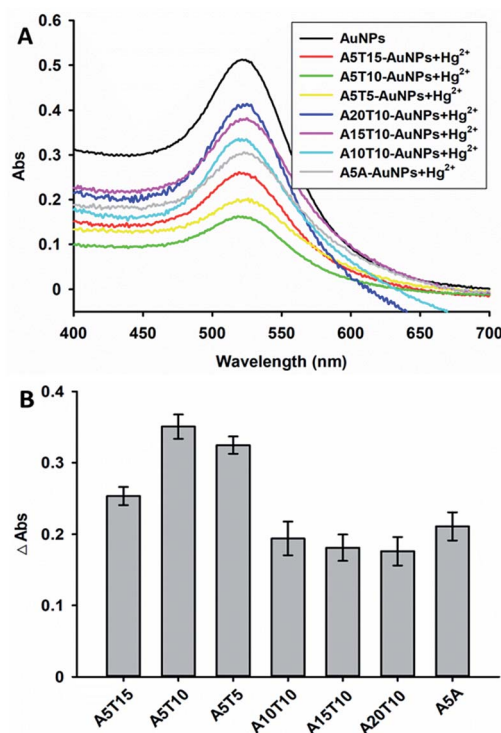**Fig. 1** The feasibility of the designed strategy specific to Hg^{2+} ions was investigated by the absorption spectrum (A) and TEM images (B) scale bar is 50 nm. Inset: the image of the corresponding solution. The concentration of Hg^{2+} ions was 1 μM.

Fig. 2 The number of adenine and thymine was optimized with adding 5 μM Hg^{2+} ions. (A) The UV-vis spectroscopy and (B) corresponding histogram.
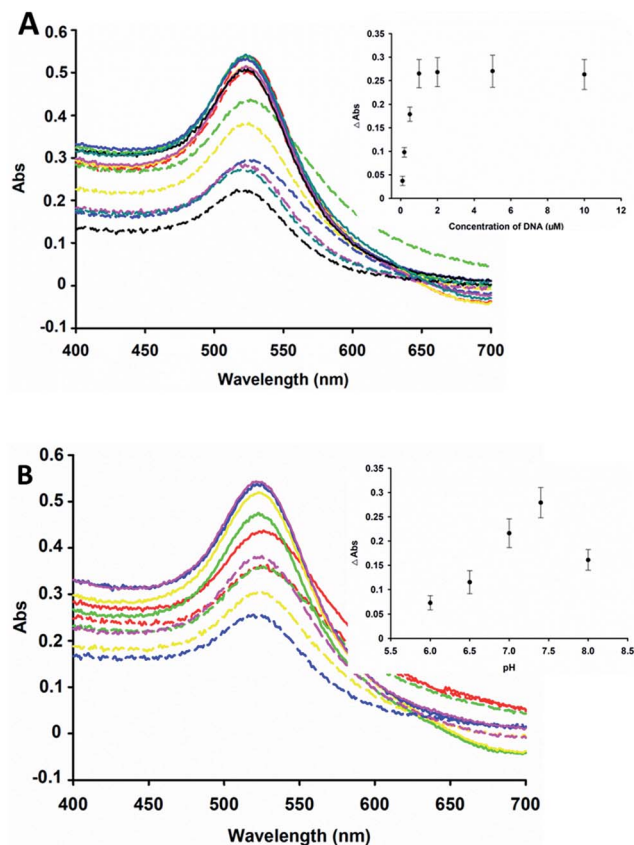
Fig. 3 The optimization of the concentrations of DNA (A) and pH effects (B) in the presence of 500 nM Hg^{2+} ions. In (A), the spectrum of each concentration of DNA used was described by full line (without Hg^{2+} ions) and dot-dashed line (with Hg^{2+} ions). The concentration of DNA: red: 0.1 μM, green: 0.2 μM, yellow: 0.5 μM, blue: 1 μM, pink: 2 μM, black: 5 μM and cyan: 10 μM. In (B), the spectrum of each pH used was described by full line (without Hg^{2+} ions) and dot-dashed line (with Hg^{2+} ions). Red: 6.0, green: 6.5, yellow: 7.0, blue: 7.4, pink: 8.0.

Sensitivity and selectivity

With optimized detection conditions, a series of samples with different concentrations (0, 5 nM, 10 nM, 20 nM, 50 nM, 100 nM, 200 nM, 500 nM, 1 μM, 5 μM and 10 μM) of Hg^{2+} ions were measured by this method. The absorbance at 520 nm gradually decreased when the amount of Hg^{2+} ions increased (Fig. 4A). For each sample, the change in the absorbance at 520 nm, Y, was plotted *versus* the concentration of Hg^{2+} ions, X, as shown in Fig. 4B. The regression equation of $Y = 0.0005X + 0.0614$ with a linear range was observed in the presence of 5–200 nM Hg^{2+} ions ($R^2 = 0.9747$). The detection limit of this method was found to be 3.75 nM, and was estimated based on the 3δ/slope rule. Compared to other colorimetric methods for the assay of Hg^{2+} ions,[10,36,37] this proposed strategy was shown to have a comfortable limit of detection based on a very facile experimental process.

In addition, the selectivity of the designed assay was also evaluated for the determination of other metal ions, including Zn^{2+}, Mn^{2+}, Cd^{2+}, Cr^{3+}, Mg^{2+}, Al^{3+}, Cu^{2+}, Ni^{2+}, Fe^{3+}, Ca^{2+}, and Pb^{2+} ions instead of Hg^{2+} ions in the solution. Fig. 5A shows the

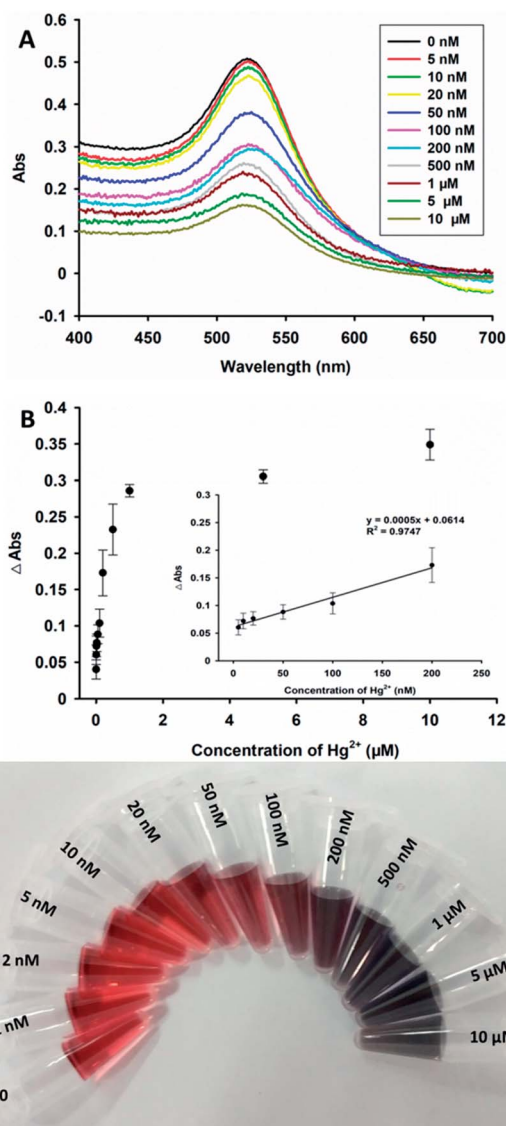**Fig. 4** (A) The UV-vis spectra of this strategy response to Hg^{2+} ions concentration (up to down: 0, 5 nM, 10 nM, 20 nM, 50 nM, 100 nM, 200 nM, 500 nM, 1 μM, 5 μM, 10 μM). (B) Absorbance value at 520 nm *versus* different concentrations of Hg^{2+} ions. Inset: the derived calibration curve. (C) The images of this strategy with different concentrations of Hg^{2+} ions.

changes in absorbance at 520 nm of this system when it was treated with different metal ions. An obvious change was observed from the solution in the presence of 1 μM Hg^{2+} ions, while very low changes were observed in the presence of other metal ions (10 μM). Thus, the results proved that the detection method has high selectivity for Hg^{2+} ions.

Detection of Hg^{2+} ions in real samples

Furthermore, the developed colorimetric assay was applied to the determination of Hg^{2+} ions in real samples, the tap water and the lake water (treated by the method mentioned in Experimental section) to realize its applicability for real sample analysis. The results are shown in Table 2, and the recovery
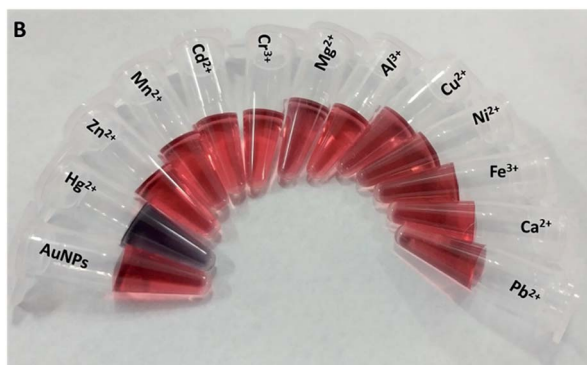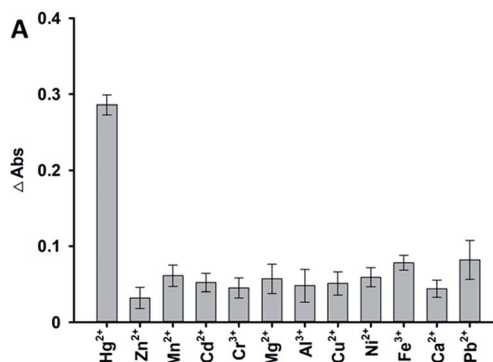
Fig. 5 (A) This method was used to detect some metal ions, including Hg^{2+}, Zn^{2+}, Mn^{2+}, Cd^{2+}, Cr^{3+}, Mg^{2+}, Al^{3+}, Cu^{2+}, Ni^{2+}, Fe^{3+}, Ca^{2+}, Pb^{2+} ions. (B) Corresponding images. The concentration of Hg^{2+} ions was 1 μM, and other metal ions were all 10 μM.

Table 2 Determination of Hg^{2+} ions in polluted water samples ($n = 3$)

Added (nM)	ICP-MS (nM)	Mean found (nM)	Recovery (%)
50	49	46	92
200	204	195	97.5
500	508	526	105.2

values ranged from 92 to 105.2% using our designed method. The excellent accuracy of this assay indicates that its application to real samples would be ideal.

Conclusions

In this work, we have developed a facile and sensitive colorimetric assay for the specific detection of Hg^{2+} ions based on poly-A mediated DNA-functionalized Au NPs. A poly-A and T-rich DNA sequence was selected to engineer the strategy for determination of Hg^{2+} ions. Poly-A was used to bring the T-rich portion onto the surface of Au NPs, and then binding specifically occurred between the T-rich portion of the oligonucleotide and the Hg^{2+} ions to form the complex of "T–Hg^{2+}–T" among the Au NPs. The color of the solution then changed from wine red to grayish blue. Under optimized detection conditions, this method can detect Hg^{2+} ions with a LOD of 3.75 nM Hg^{2+} ions in a linear range from 5 nM to 200 nM by using UV-Vis

spectroscopy. Furthermore, this method had good accuracy that can be applied to real samples. Thus, a simple and low-cost colorimetric assay for Hg^{2+} ions with high sensitivity and selectivity was developed that has great potential for monitoring Hg^{2+} ions in the environment.

Conflicts of interest

There are no conflicts to declare.

Acknowledgements

Notes and references

1 T. W. Clarkson and L. Magos, *Crit. Rev. Toxicol.*, 2006, **36**, 609–662.

2 H. H. Harris, I. J. Pickering and G. N. George, *Science*, 2003, **301**, 1203.

3 Z. Gu, M. X. Zhao, Y. W. Sheng, L. A. Bentolila and Y. Tang, *Anal. Chem.*, 2011, **83**, 2324–2329.

4 Y. Choi, Y. Park, T. Kang and L. P. Lee, *Nat. Nanotechnol.*, 2009, **4**, 742–746.

5 E. S. Cho, J. Kim, B. Tejerina, T. M. Hermans, H. Jiang, H. Nakanishi, M. Yu, A. Z. Patashinski, S. C. Glotzer and F. Stellacci, *Nat. Mater.*, 2012, **11**, 978–985.

6 Z. B. Chen, C. M. Zhang, Q. G. Gao, G. Wang, L. L. Tan and Q. Liao, *Anal. Chem.*, 2015, **87**, 10963–10968.

7 C. Yuan, B. Liu, F. Liu, M. Y. Han and Z. Zhang, *Anal. Chem.*, 2014, **86**, 1123–1130.

8 J. Du, B. Zhu and X. Chen, *Small*, 2013, **9**, 4104–4111.

9 X. Li, J. Q. Xie, B. Y. Jiang, R. Yuan and Y. Xiang, *ACS Appl. Mater. Interfaces*, 2017, **9**, 5733–5738.

10 L. L. Tan, Z. B. Chen, C. Zhang, X. C. Wei, T. H. Lou and Y. Zhao, *Small*, 2017, **13**, 1603370–1603377.

11 Q. F. Zhai, H. H. Xing, X. W. Zhang, J. Li and E. K. Wang, *Anal. Chem.*, 2017, **89**, 7788–7794.

12 G. Aragay, J. Pons and A. Merkoçi, *Chem. Rev.*, 2011, **111**, 3433–3458.

13 Z. H. Fernández, L. A. V. Rojas, A. M. Álvarez, J. R. E. Álvarez, J. A. dos Santos, I. P. González, M. R. Gonzalez, N. A. Macias, D. L. Sanchez and D. H. Torres, *Food Control*, 2015, **48**, 37–42.

14 M. Noël, J. R. Christensen, J. Spence and C. T. Robbins, *Sci. Total Environ.*, 2015, **529**, 1–9.

15 W. N. Chen, S. J. Jiang, Y. L. Chen and A. C. Sahayam, *Anal. Chim. Acta*, 2015, **860**, 8–14.

16 J. T. Petty, J. Zheng, N. V. Hud and R. M. Dickson, *J. Am. Chem. Soc.*, 2004, **126**, 5207–5212.

17 N. Ma, E. H. Sargent and S. O. Kelley, *Nat. Nanotechnol.*, 2009, **4**, 121–125.

18 A. Lopez and J. W. Liu, *Can. J. Chem.*, 2015, **93**, 615–620.

19 S. J. Reinholt and H. G. Craighead, *Anal. Chem.*, 2018, **90**, 2601–2608.

20 P. F. Zhang, Z. Zhao, C. S. Li, H. F. Su, Y. Y. Wu, R. T. K. Kwok, J. W. Y. Lam, P. Gong, L. T. Cai and B. Z. Tang, *Anal. Chem.*, 2018, **90**, 1063–1067.

21 J. J. Yin, Y. Q. Liu, S. Wang, J. K. Deng, X. D. Lin and J. T. Gao, *Sens. Actuators, B*, 2018, **256**, 573–579.

22 Y. Miyake, H. Togashi, M. Tashiro, H. Yamaguchi, S. Oda, M. Kudo, Y. Tanaka, Y. Kondo, R. Sawa, T. Fujimoto, T. Machinami and A. Ono, *J. Am. Chem. Soc.*, 2006, **128**, 2172–2173.

23 X. Y. Jiang, H. J. Wang, H. J. Wang, R. Yuan and Y. Q. Chai, *Anal. Chem.*, 2016, **88**, 9243–9250.

24 X. J. Liu, Z. J. Wu, Q. Q. Zhang, W. F. Zhao, C. H. Zong and H. W. Gai, *Anal. Chem.*, 2016, **88**, 2119–2124.

25 B. Liu, *Biosens. Bioelectron.*, 2008, **24**, 756–760.

26 M. Annadhasan, T. Muthukumarasamyvel, V. R. Sankar Babu and N. Rajendiran, *ACS Sustainable Chem. Eng.*, 2014, **2**, 887–896.

27 Y. Zhao, L. L. Gui and Z. B. Chen, *Sens. Actuators, B*, 2017, **241**, 262–267.

28 X. F. Ding, L. T. Kong, J. Wang, F. Fang, D. D. Li and J. H. Liu, *ACS Appl. Mater. Interfaces*, 2013, **5**, 7072–7078.

29 J. S. Lee, M. S. Han and C. A. Mirkin, *Angew. Chem., Int. Ed.*, 2007, **46**, 4093–4096.

30 X. J. Xue, F. Wang and X. G. Liu, *J. Am. Chem. Soc.*, 2008, **130**, 3244–3245.

31 T. T. Lou, Z. P. Chen, Y. Q. Wang and L. X. Chen, *ACS Appl. Mater. Interfaces*, 2011, **3**, 1568–1573.

32 J. W. Liu and Y. Lu, *Nat. Protoc.*, 2006, **1**, 246–252.

33 A. Opdahl, D. Y. Petrovykh, H. K. Suda, M. J. Tarlov and L. J. Whitman, *Proc. Natl. Acad. Sci. U. S. A.*, 2007, **104**, 9–14.

34 D. Zhu, P. Song, J. W. Shen, S. Su, J. Chao, A. Aldalbahi, Z. A. Zhou, S. P. Song, C. H. Fan, X. L. Zuo, Y. Tian, L. H. Wang and H. Pei, *Anal. Chem.*, 2016, **88**, 4949–4954.

35 H. D Hill and C. A. Mirkin, *Nat. Protoc.*, 2006, **1**, 324–336.

36 Z. H. Qing, X. X. He, K. M. Wang, Z. Z. Zou, X. Yang, J. Huang and G. P. Yan, *Anal. Methods*, 2012, **4**, 3320–3325.

37 W. H. Ni, H. J. Chen, J. Su, Z. H. Sun, J. F. Wang and H. K. Wu, *J. Am. Chem. Soc.*, 2010, **132**, 4806–4814.